




The role of noise in the tumor dynamics under chemotherapy treatment

Irina Bashkirtseva¹, Lev Ryashko¹, Jorge Duarte^{2,3}, Jesús M. Seoane^{4,a} , Miguel A. F. Sanjuan⁴

¹ Institute of Mathematics and Computer Sciences, Ural Federal University, Lenina, 51, Ekaterinburg, Russia 620000

² Department of Mathematics, ISEL-Engineering Superior Institute of Lisbon, Rua Emídio Navarro 1, 1950-007 Lisboa, Portugal

³ Center for Mathematical Analysis, Geometry and Dynamical Systems, Instituto Superior Técnico, Universidade de Lisboa, Lisboa, Portugal

⁴ Nonlinear Dynamics, Chaos and Complex Systems Group, Departamento de Física, Universidad Rey Juan Carlos, Tulipán s/n, Móstoles, Madrid 28933, Spain

Received: 26 June 2021 / Accepted: 11 October 2021

© The Author(s) 2021

Abstract Dynamical systems modeling tumor growth have been investigated to analyze the dynamics between tumor and healthy cells. Recent theoretical studies indicate that these interactions may lead to different dynamical outcomes under the effect of particular cancer therapies. In the present paper, we derive a system of nonlinear differential equations, in order to investigate solid tumors *in vivo*, taking into account the impact of chemotherapy on both tumor and healthy cells. We start by studying our model only in terms of deterministic dynamics under the variation of a drug concentration parameter. Later, with the introduction of noise, a stochastic model is used to analyze the impact of the unavoidable random fluctuations. As a result, new insights into noise-induced transitions are provided and illustrated in detail using techniques from dynamical systems and from the theory of stochastic processes.

1 Introduction

The term *cancer* designates generically a group of diseases involving abnormal cell growth with the potential for spreading to new locations and invade other parts of the body. This process contrasts with benign tumors, which do not spread. Cancer can be detected by certain signs and symptoms or screening tests. Nevertheless, despite the encouraging progresses, we have only a limited understanding of cancer and there is no known effective cure for the disease [1]. As a matter of fact, in 2015, about 90.5 million people had cancer. In very recent years, annually, it caused about 8.8 million deaths (15.7% of deaths) (additional information can be found in [2] and [3]). Metastasis is the spread of cancer to other locations in the body. The dispersed tumors are called metastatic tumors. As a matter of fact, most cancer deaths are due to cancer that has metastasized. In order to control this tragic outcome, different types of therapeutic methodologies have been adopted by oncologists, such as surgery, radiotherapy,

^a e-mail: jesus.seoane@urjc.es (corresponding author)

anti-angiogenic drugs, immunotherapy, chemotherapy, among others. The chance of survival depends on the type of cancer and extent of disease at the start of treatment.

In order to gain revealing insights into important phenomena involved in tumor growth and to predict its future behavior, different cancer models have been used. Complex interactions among different body cells, namely tumor cells, healthy tissue cells and activated immune cells, are considered in the modeling process, which usually includes a treatment strategy. Key factors that influence the treatment choice are: tumor severity, age, sex and immune system state of the patient. It has been shown in the literature that cancer growth models are particularly complex in its dynamics (see, for instance, [1, 4, 5] and references therein).

Depending on the type of cancer and stage, particularly when cells seem to be resistant to immune elimination ([6, 7]), chemotherapy is often applied against tumor progression. Even with their limitations and side effects, chemotherapy may be useful to reduce symptoms such as pain or to reduce the size of an inoperable tumor in the hope that surgery will become possible in the future. It is a fact that the application of chemotherapy remains an important and sensitive research topic to improve [8].

In order to study the reduction of tumor population in an optimal manner, particular treatment protocols, mainly chemotherapy, immunotherapy or radiotherapy, have been taken into consideration on cancer models. Some recent works have focused their attention on solid tumors *in vitro* [9].

In the present study, with the purpose of enhancing our understanding of tumor growth *in vivo* in the presence of traditional therapies, we will be concerned with the effect of chemotherapy on both the healthy tissue and tumor cells. In particular, our main goal is to illustrate in simple terms and to provide insights into the dynamical effect of adding noise to a two-dimensional deterministic model, studying a stochastic system under the usage of chemotherapy. More specifically, these insights correspond to a deeper understanding and a wider perspective into the different dynamical scenarios that can emerge from the suggested numerical simulations in a stochastic context, when noise is added to a deterministic system. Accordingly, as a contribution to the literature, we will discuss the use of bifurcation analysis to design treatment protocols of different stages. More precisely, the values of specific parameters at the bifurcation points are biologically meaningful and will offer us the possibility for recognizing the sufficient drug concentration to be used in order to suppress tumor cells. In fact, throughout our work, the bifurcation values of the drug concentration C , precisely $C = C_1$ and $C = C_2$, allow us to characterize dynamical scenarios corresponding to $C < C_1$, $C_1 < C < C_2$ and $C > C_2$ that guide the entire discussion on the impact of the considered noise intensity. Biologically speaking, this noise intensity corresponds to the amount of random variability in different quantities (e.g., dynamical variables and parameters) arising in cellular biology.

The subsequent part of this article is organized as follows. In Sect. 2, we describe the basic features and dynamical properties of the deterministic version of the model. Divided into two subsections, Sect. 3 is devoted to the analysis of the main topic of the present work—the stochastic effects on the tumor growth model provided by the noise-induced dynamics. The closing Sect. 4 is devoted to the usual final considerations about the undertaken study.

2 Deterministic model

The mathematical model that we are using was developed in [10], and it corresponds to the one described in [11], though no constant input of effector immune cells is considered. Each variable represents a cell population, where $T(t)$ corresponds to the tumor cells, $H(t)$ to the

healthy host cells, and $E(t)$ to the effector immune cells. The growth of cancer and host cells follows a logistic curve with growth rate r_i and carrying capacity k_i . As a competitive model, the parameters a_{ij} represent the competitive parameters.

The parameter r_3 represents the immune effector cell production rate related to the response of the presence of tumor cells. On the other hand, k_3 corresponds to the steepness of the response curve; that is, the value of the tumor cells at which the immune response rate is half of the maximum production, threshold for which the response curve saturates. Immune effector cells only compete with cancer cells. In the absence of these cells, they die off with a constant per capita rate d_3 . Thus, the system reads as follows:

$$\begin{aligned} \dot{T} &= r_1 T \left(1 - \frac{T}{k_1}\right) - a_{12} T H - a_{13} T E \\ \dot{H} &= r_2 H \left(1 - \frac{H}{k_2}\right) - a_{21} H T \\ \dot{E} &= r_3 \frac{ET}{T + k_3} - a_{31} E T - d_3 E. \end{aligned} \tag{1}$$

The nondimensionalization and parameter reduction of this system is thoroughly studied in [5, 10], yielding the set of equations

$$\begin{aligned} \dot{x} &= x(1 - x) - a_{12}xy - a_{13}xz \\ \dot{y} &= r_2y(1 - y) - a_{21}yx \\ \dot{z} &= r_3 \frac{zx}{x + k_3} - a_{31}zx - d_3z, \end{aligned} \tag{2}$$

where x is the density of population of tumor cells, y is the density of population of healthy cells, z is the density of population of immune cells, and $a_{12}, a_{13}, a_{21}, a_{31}, r_2, r_3$ and d_3 are the dimensionless parameters of the system. For our purpose, we take the two-dimensional system obtained after making $z = 0$ from Eq. 2. This means that we do not consider the existence of the immune cells. In this situation, our system can be written as

$$\begin{aligned} \dot{x} &= x(1 - x) - a_{12}xy \\ \dot{y} &= ry(1 - y) - a_{21}xy, \end{aligned} \tag{3}$$

where we fix the parameters $a_{12} = 0.5, a_{21} = 4.8$ and $r_2 = r = 1.2$ following [12].

On the other hand, to take into account the impact of chemotherapy, we follow the fractional cell kill law used in [9] and derive the model

$$\begin{aligned} \dot{x} &= x(1 - x) - \frac{a(1 - e^{-\rho_1 C})x}{1 + s_1x} - a_{12}xy \\ \dot{y} &= ry(1 - y) - a_{21}xy - \frac{b(1 - e^{-\rho_2 C})y}{1 + s_2y} \end{aligned} \tag{4}$$

where the dynamical variables and parameter values are listed and described in Table 1. Terms associated with the treatment contain six parameters: $a, b, \rho_1, \rho_2, s_1$ and s_2 , which have no units since they are dimensionless quantities. We suppose $a \gg b$, because the tumor must be more sensitive to drugs than the healthy cells. The behavior of Eq. 4 is studied under a variation of the parameter C of the drug concentration. Notice that, in the context of our study, we do not need to pay attention with the pharmacokinetics of the drug itself since here the drug concentration is treated as a parameter. As far as the administration of chemotherapy is concerned, this model allows us to represent the so-called Norton–Simon hypothesis. As

Table 1 Description of the dynamical variables and parameters of the model of Eq. 3 and their values

Variables/Parameters	Biological meaning	Default values
x	Density of tumor cells	
y	Density of healthy cells	
a	Relative maximum fractional tumor cell kill	2
b	Relative maximum fractional healthy cell kill	0.1
ρ_1	Sensitivity of the tumor cells to the drugs	1.0
ρ_2	Sensitivity of the healthy cells to the drugs	2.0
s_1, s_2	Control of the extent to which the Norton–Simon effect is operating	1.0
a_{12}	Tumor cells inactivation rate by the healthy cells	0.5
a_{21}	Healthy cells inactivation rate by the tumor cells	4.8
r	Intrinsic growth rate of the healthy tissue cells	1.2
C	Drug concentration (control parameter under study)	

Notice that both the variables and the parameters have not units since they are dimensionless quantities

pointed out in [9], this hypothesis states that the rate of destruction of a cytotoxic agent is proportional to the rate of growth of the unperturbed tissue (tumor cells/healthy cells). The fractional cell kill by cytotoxic agents can then be described by means of an exponential kill model, which has been tested against experimental results. This model describes the rate of cell kill by using the mathematical functions $a(1 - e^{-\rho_1 C})$ and $b(1 - e^{-\rho_2 C})$, corresponding to the tumor cells and healthy tissue, respectively.

In order to gain direct insights into the dynamics of the system in the absence of noise, we first examine the equilibria and perform a phase plane analysis, having C as the most relevant parameter. Indeed, Eq. 3 possesses several equilibrium points called $M_n(x, y)$ where $n = 0, 1, 2$. The trivial one, $M_0(0, 0)$, is unstable for the considered choice of parameters. On the other hand, coordinates of equilibria $M_1(x, 0)$ and $M_2(0, y)$ can be obtained from the equations:

$$(1 - x)(1 + s_1x) - a(1 - e^{-\rho_1 C}) = 0, \tag{5}$$

$$r(1 - y)(1 + s_2y) - b(1 - e^{-\rho_2 C}) = 0. \tag{6}$$

Here, we consider only nonnegative roots; that is, the ones that are biologically meaningful. For $s_1 = s_2 = 1$, we have:

$$x = \sqrt{1 - a(1 - e^{-\rho_1 C})}, \quad y = \sqrt{1 - \frac{b(1 - e^{-\rho_2 C})}{r}}. \tag{7}$$

Moreover, the system can possess the equilibrium point $M_3(x, y)$ in which $x, y > 0$ and they are governed by the equations:

$$r(1 - \varphi(x)) - \frac{b(1 - e^{-\rho_2 C})}{1 + s_2\varphi(x)} - a_{21}x = 0, \quad y = \varphi(x), \tag{8}$$

where

$$\varphi(x) = \frac{(1 - x)(1 + s_1x) - a(1 - e^{-\rho_1 C})}{(1 + s_1x)a_{12}}. \tag{9}$$

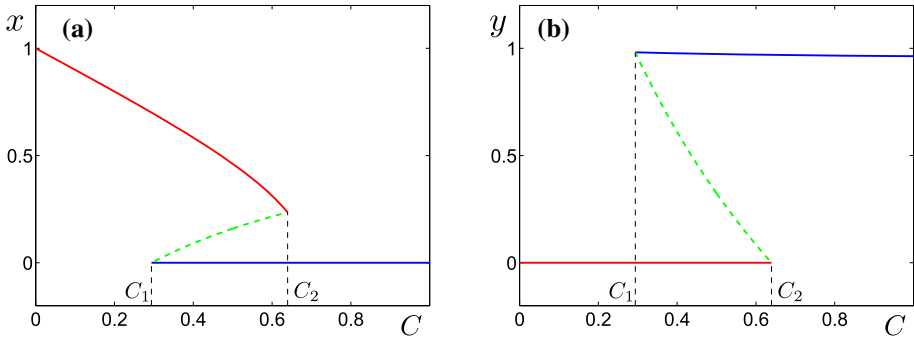


Fig. 1 Bifurcations diagrams versus parameter C of drug concentration. **a** Bifurcation diagram of the variable x versus C . **b** Bifurcation diagram of the variable y versus C . We have fixed the rest of the parameter values as $a = 2, b = 0.1, \rho_1 = 1, \rho_2 = 2, s_1 = s_2 = 1$

We evaluate now how the chemotherapy with increasing drug concentration C affects the changes in the density of tumor cells x and in the density of healthy cells y . The key dynamical regimes of Eq. 4 under the variation of C in the interval $0 \leq C \leq 1$ are well seen in the bifurcation diagram shown in Fig. 1. Here, $C_1 = 0.2939$ and $C_2 = 0.6394$ are bifurcation points. The equilibrium M_1 (red color) is stable in the interval $0 \leq C < C_2$. The equilibrium M_2 (blue color) is stable in the interval $C_1 < C \leq 1$. The equilibrium M_1 corresponds, according to [9], to the state of an *active tumor* (AT), while M_2 stands for the *dead tumor* (DT).

Three dynamical regimes can be described in biological terms: (i) in the interval $0 \leq C < C_1$, that can be interpreted as *weak therapy*, Eq. 4 is monostable—independently of the initial state, the system transits to the state of AT; (ii) in the interval $C_2 < C \leq 1$ of the *strong therapy*, the system is also monostable, and all solutions tend to the state of DT; (iii) in the interval $C_1 < C < C_2$ of *intermediate strength of therapy*, the system (4) is bistable: situation where both regimes, AT and DT, coexist. Depending on the ratio of the tumor and healthy cells, the solution converges either to M_1 (AT) or to M_2 (DT). These two equilibria, M_1 and M_2 , are biologically meaningful. The active tumor (AT) equilibrium corresponds to a malignant attractor for which the tumor has an unacceptable level of tumor cells and can develop an increased metastatic potential. Actually, the DT equilibrium represents the tumor extinction.

For the three dynamical scenarios above mentioned, phase portraits are shown in Fig. 2 for different values of the drug concentration C , namely for $C = 0.2$ (AT), $C = 0.5$ (AT + DT) and $C = 0.7$ (DT). In the bistability case (Fig. 2b), the saddle equilibrium M_3 (empty point) plays an important role: its stable manifold (green dashed) separates basins of attraction of the stable equilibria M_1 and M_2 .

Based on results of the bifurcation analysis depicted in Fig. 1, the following *protocol of two-stage treatment* can be proposed. At the *first stage*, we use drug concentration slightly above C_2 . This allows us to suppress tumor cells independently of the initial values of tumor and healthy cells. In the *second stage*, to provide this state of DT, it is sufficient to use drugs with concentration C slightly above C_1 . Such a protocol of treatment is valid only from the point of view of the deterministic model, since the presence of random disturbances can significantly change the behavior comparing with the deterministic prediction.

At this moment of our study, and in the sequence of the previous deterministic approach, it is necessary to consider the dynamical behavior of system of Eq. (4) under the effect of

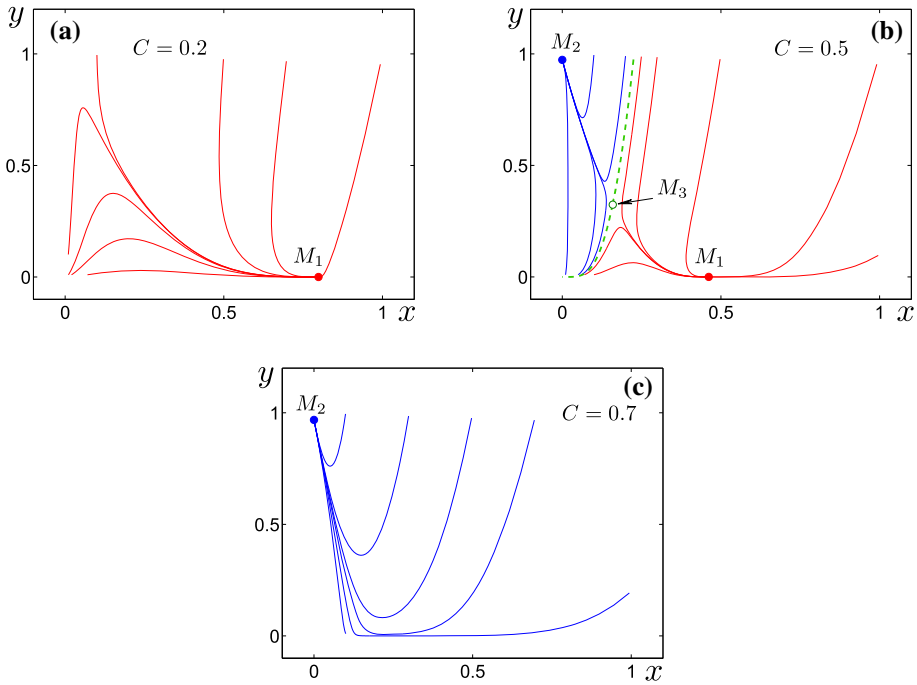


Fig. 2 The figure shows the phase portraits of Eq. (4) for different values of the drug concentration C . We have fixed the rest of the parameters as $a = 2, b = 0.1, \rho_1 = 1, \rho_2 = 2, s_1 = s_2 = 1$. **a** $C = 0.2$, **b** $C = 0.5$, and **c** $C = 0.7$

random disturbances, since the tumor growth does not usually take place in a deterministic manner.

3 Stochastic model

To study the impact of random fluctuations, we will use the following stochastic model

$$\begin{aligned} \dot{x} &= x(1 - x) - \frac{a(1 - e^{-\rho_1 C})x}{1 + s_1 x} - a_{12}xy + \varepsilon_1 \xi_1(t) \\ \dot{y} &= ry(1 - y) - a_{21}xy - \frac{b(1 - e^{-\rho_2 C})y}{1 + s_2 y} + \varepsilon_2 \xi_2(t). \end{aligned} \tag{10}$$

Here, $\xi_1(t)$ and $\xi_2(t)$ are uncorrelated Gaussian white noises with values of noise intensity ε_1 and ε_2 . In what follows, we consider $\varepsilon_1 = \varepsilon_2 = \varepsilon$ and use a Euler–Maruyama scheme [13] with the time step 10^{-3} for numerical simulation of the random solutions. With the purpose of preserving both the physical and the biological sense, we have to keep the variables x and y nonnegative and use a corresponding truncation procedure. Different dynamical scenarios can emerge in a stochastic context, as a result of adding noise to a deterministic system. In this sense, some recent works have been focused on the influence of random fluctuations on the recruitment of effector cells toward a tumor (please see [5, 14] and references therein). For the sake of clarity, the following subsections are devoted to noise-induced dynamical scenarios of different nature.

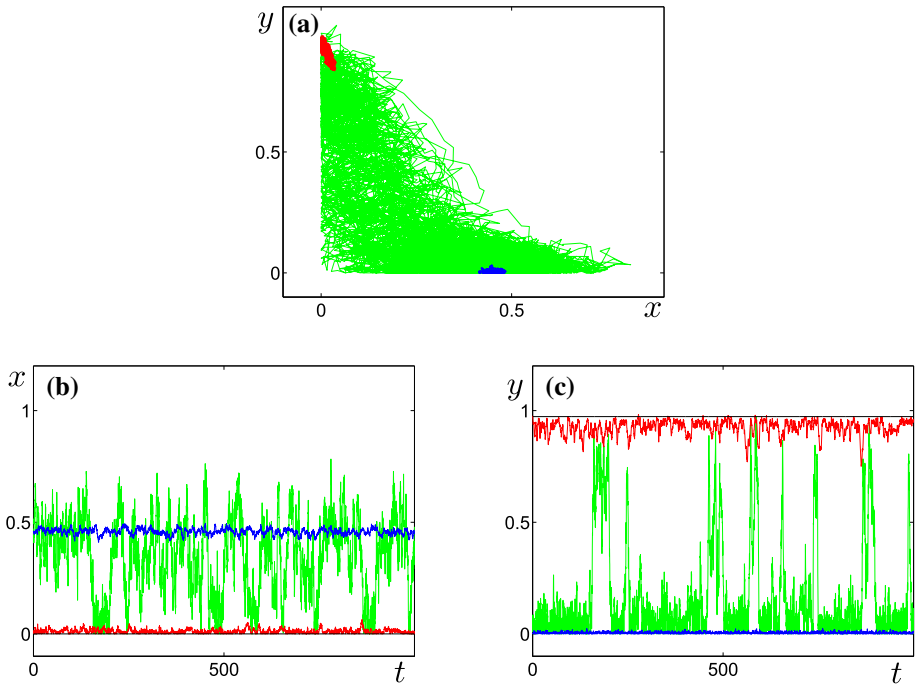


Fig. 3 **a** The figure represents a stochastic trajectory in phase space **b** Time series of the stochastic model Eq. 10 with $C = 0.5$ and $\varepsilon = 0.01$ (blue for M_1 and red for M_2) **c** Time series of the stochastic model, Eq. 10 with $C = 0.5$ and $\varepsilon = 0.1$ (green)

3.1 Noise-induced transitions in the bistability zone

Firstly, we consider the influence of noise in the parameter zone $C_1 < C < C_2$, where Eq. 4 possesses two stable equilibria, M_1 and M_2 . Results of our stochastic modeling are presented in Fig. 3 for $C = 0.5$ and two values of the noise intensity. For an initial value of noise $\varepsilon = 0.01$ random trajectories starting from M_1 (blue) and M_2 (red) exhibit small-amplitude noisy fluctuations near the initial deterministic equilibria.

For increasing values of noise, the solutions start to intersect the separatrix between basins of coexisting equilibria, transiting between these basins. Such intermittent behavior is shown in green color in Fig. 3 for $\varepsilon = 0.1$. Here, three stages can be seen: (i) small-amplitude stochastic oscillations in the basin of M_1 ; (ii) small-amplitude stochastic oscillations in the basin of M_2 and (iii) large-amplitude jumps between basins.

Details of noise-induced transformations of the dynamics of Eq. 10 are shown in Figs. 4–5 for different values of the drug concentration C within the bistability zone. In these two figures, random states of the system of Eq. 10 for solutions starting from M_1 (AT) are shown in red color and for solutions starting from M_2 (DT) are plotted in blue color. Corresponding mean values of the densities x and y , varying the noise intensity ε , are shown in light blue.

As we can see, near the left point $C_1 = 0.2939$ of the bistability interval (see Fig. 4 for $C = 0.3$), firstly increasing noise induces one-way transitions from M_2 to M_1 . Therefore, among coexisting stable equilibria M_1 and M_2 , we can observe how the noise induces the tumor into the state of active tumor. With further increase in the noise intensity ε , the stochastic system exhibits an intermittency with repetitive transitions between M_1 and M_2 .

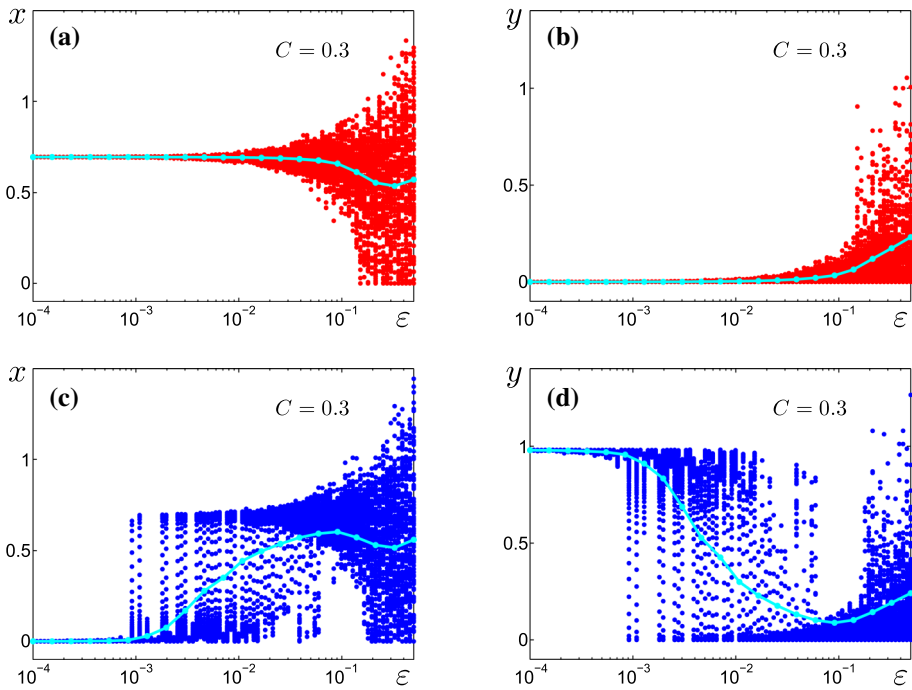


Fig. 4 Random states of the variables x and y described in the stochastic model, Eq. 10, versus ε with $C = 0.3$. In figures **a** and **b**, the trajectories start from M_1 (AT), while in figures **c** and **d** start from M_2 (DT). The mean values, plotted by a light blue color, are calculated over a period of $t = 100$

Near the right point $C_2 = 0.6394$ (see Fig. 5 for $C = 0.63$), before the onset of stochastic mixing, the system demonstrates noise-induced transition to the state of M_2 (DT).

3.2 Noise-induced excitement in the monostability zone

Now, let us consider the influence of noise in the parameter zone $C > C_2$, where the system described in Eq. 4 possesses a single stable equilibrium M_2 corresponding to the state of DT.

For that purpose, we plot Figs. 4, 5 and 6. In Fig. 6, random states (blue) of the stochastic system starting from M_2 are plotted versus the noise intensity along with the mean values of the dynamical variables x and y (light blue).

Even in the monostable system with a singular equilibrium, large-amplitude stochastic oscillations can be induced by noise with increasing intensity. An example of a such excitement is shown in Fig. 7, where time series of stochastic solutions starting from M_2 are plotted for $C = 0.7$ and $\varepsilon = 0.01$ (blue), $\varepsilon = 0.1$ (green). As we can observe, for $\varepsilon = 0.01$ the system shows small-amplitude noisy oscillations near M_2 . For a larger intensity noise, $\varepsilon = 0.1$, the system exhibits large-amplitude spiking oscillations of complex form.

The transition from small- to large-amplitude stochastic oscillations with increasing noise are accompanied by the significant changes of the form of the probability density. In Fig. 8, one can see these changes for $C = 0.64$ and $C = 0.7$ under increasing values of ε .

Here, it should be noted that the form of the probability density function of the variable y , $p(y)$, changes its modality: one peak \rightarrow two peaks \rightarrow one peak. Such a qualitative deformation of the form of $p(y)$ is commonly interpreted as an stochastic P -bifurcation.

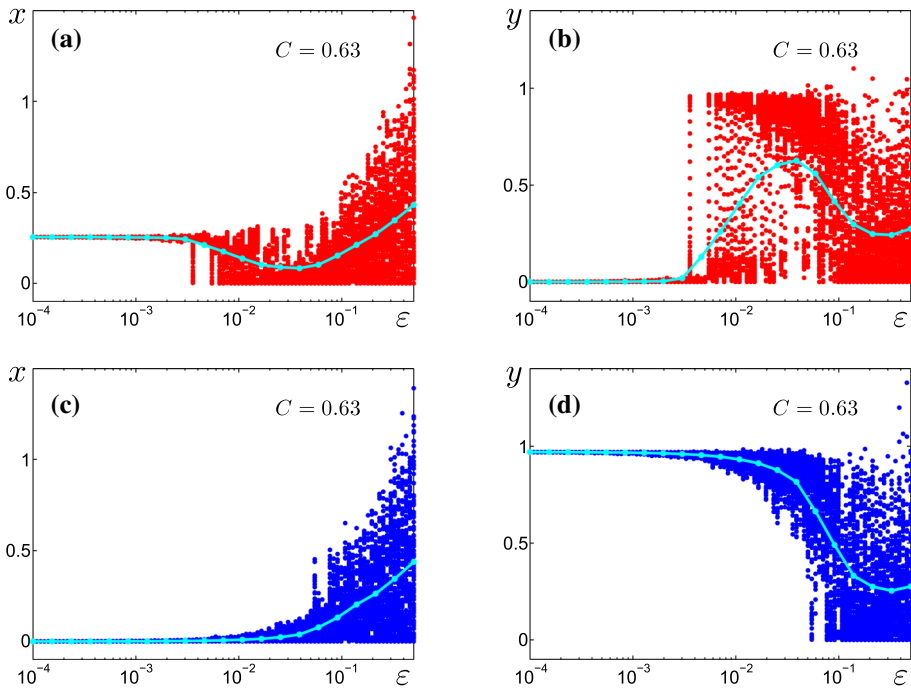


Fig. 5 Random states of the variables x and y described in the stochastic model, Eq. 10, versus ε with $C = 0.63$. In figures **a** and **b**, the trajectories start from M_1 (AT), while in the figures **c** and **d** start from M_2 (DT). The mean values, plotted by a light blue color, are calculated over a period of $t = 100$

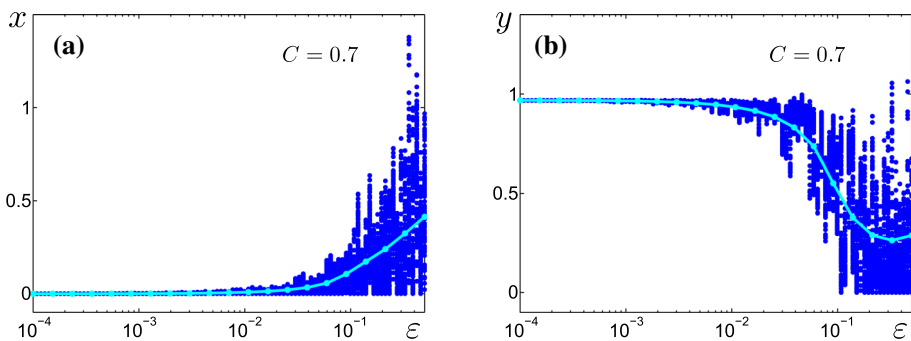


Fig. 6 Random states of the variables x and y described in the stochastic model, Eq. 10, versus ε with $C = 0.7$ starting from M_2 (DT). The mean values, plotted by a light blue color, are calculated over a period of $t = 100$

Finally, we consider how these amplitude changes are connected with the frequency characteristics. When studying spikes (which represent quantitative changes in the biological dynamical variables), the mean values of random interspike intervals (ISI), $\langle \tau \rangle$, constitute basic statistics that are worth taking in consideration. In practical terms, a short interspike interval means that it has occurred a rapid change and, similarly, a wide interspike interval means that a significant change only occurred after a long period of time. Having established that, in Fig. 9 we plot mean values of ISI, $\langle \tau \rangle$, for three values of C versus the noise intensity ε . For weak noises, i.e., low values of ε , the mean values of random interspike intervals, $\langle \tau \rangle$,

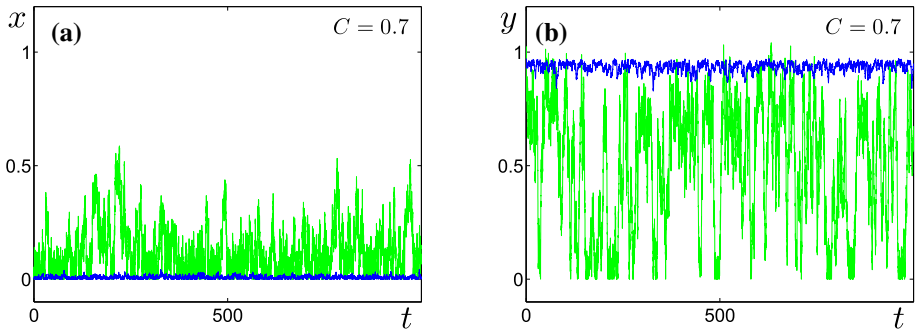


Fig. 7 Stochastic excitation. The figures show the time series of the system described in the stochastic model, Eq. 10, with $C = 0.7$ and different values of the noise intensity: $\varepsilon = 0.01$ (blue), $\varepsilon = 0.1$ (green)

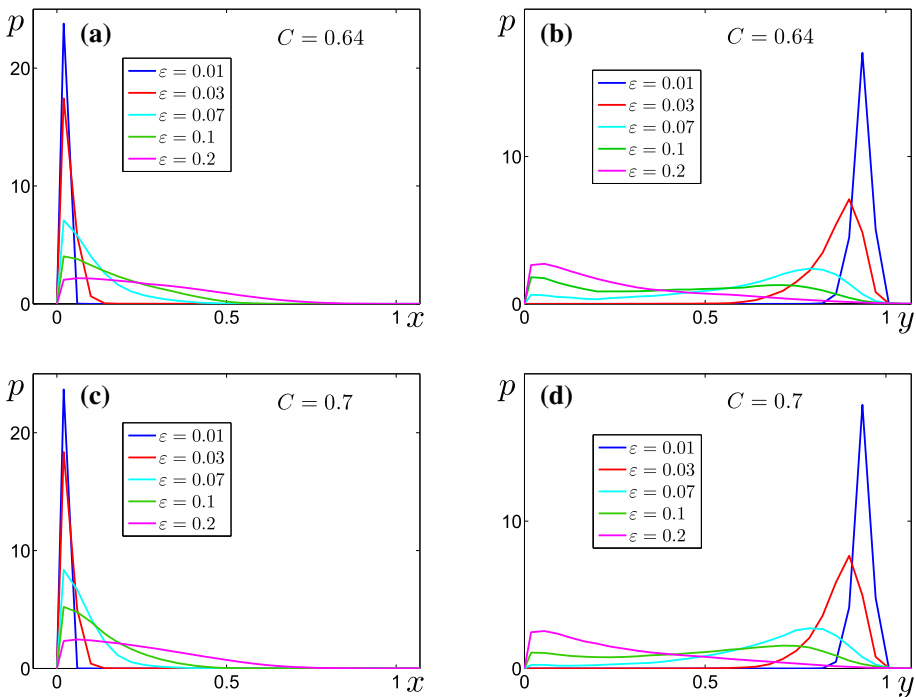


Fig. 8 Plots of the probability density functions p of the stochastic system described by Eq. 10 in function of the variables x and y for different values of the noise intensity. **a** Probability density function $p(x)$ for $C = 0.64$. **b** Probability density function $p(y)$ for $C = 0.64$. **c** Probability density function $p(x)$ for $C = 0.7$. **d** Probability density function $p(y)$ for $C = 0.7$

are higher, which indicates that spikes (biological changes) are rare. Therefore, in biological terms, sudden significant changes of the dynamical variables are only expected to occur for increasing values of the noise intensity. The ε -interval, where plots of $\langle \tau \rangle$ sharply decrease, marks the onset of the noise-induced generation of spikes. The larger the C , the stronger the noise necessary to generate the spiking regime. Biologically, this means that increasing values of the drug concentration require higher values of the noise intensity for significant changes (spikes) of the dynamical variables take place (please observe the three curves of

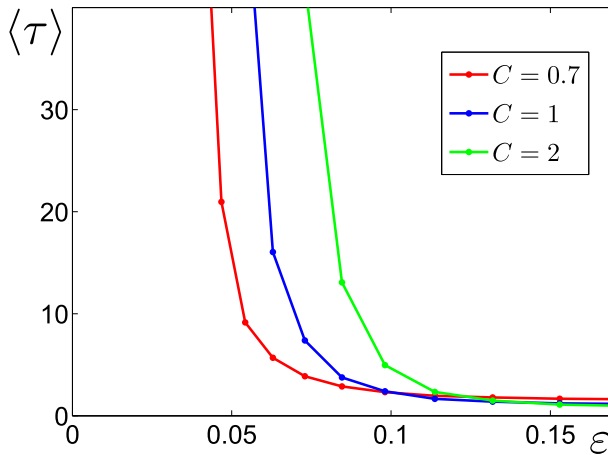


Fig. 9 Mean values of the interspike intervals, $\langle \tau \rangle$, given by the stochastic model given by Eq. 10 for $C = 0.7$ (red curve), $C = 1$ (blue curve) and $C = 1.2$ (green curve)

Fig. 9, and their corresponding ranges of values ε , for $C = 0.7$ (red curve), $C = 1$ (blue curve) and $C = 1.2$ (green curve)).

4 Concluding remarks

In order to shed light into the study of *in vivo* tumors, we have designed a two-dimensional mathematical model of nonlinear differential equations, taking into account the impact of chemotherapy on both the tumor and the healthy cells. Studying the model adopting the deterministic and the stochastic approaches allowed us to provide valuable insights into noteworthy and eye-catching features of the dynamics.

Interestingly, primary results of the deterministic bifurcation analysis lead us to immediately propose a protocol of a two-stage treatment, involving two distinct levels of drug administration. Taking into account that the tumor growth does not usually take place in a deterministic manner, the addition of noise brings more realism to our study. As a consequence, the discussion of the noise-induced dynamics of the system became particularly relevant. As a matter of fact, it is well known that stochasticity can be found at early stages of tumorigenesis.

Striking features of the dynamical behavior have been pointed out and illustrated within the framework of both the nonlinear dynamics and the theory of stochastic processes using mainly bifurcation diagrams, phase portraits, time series and probability density plots, among others. We found that the dynamics is particularly sensitive to the variation of the drug concentration (chemotherapy), as well as to the noise intensities that have been used in the problem. As a consequence, it has a very important effect on the overall dynamics of the system. In this sense, our theoretical results suggest that a careful control of these parameters from a medical point of view could have a significant role in the fate of tumor cell populations.

This study provides another illustration of how an integrated approach, involving numerical evidences and theoretical reasoning, within the theory of deterministic and stochastic systems, can contribute to our understanding of important biological models. In addition, our work aims to offer a trustworthy explanation of complex phenomena (series of chemical

reactions, among other possible events, that result in a transformation) witnessed in biological systems.

Acknowledgements The work of IB and LR on the analysis of noise-induced phenomena was supported by Russian Science Foundation (21-11-00062). The work on the deterministic analysis has been financially supported by the Portuguese Foundation for Science and Technology (FCT) under Project No. UID/MAT/04459/2013 (JD) and by the Spanish State Research Agency (AEI) and the European Regional Development Fund (ERDF, EU) under Project No. PID2019-105554GB-I00 (JMS and MAFS).

Funding Open Access funding provided thanks to the CRUE-CSIC agreement with Springer Nature.

Open Access This article is licensed under a Creative Commons Attribution 4.0 International License, which permits use, sharing, adaptation, distribution and reproduction in any medium or format, as long as you give appropriate credit to the original author(s) and the source, provide a link to the Creative Commons licence, and indicate if changes were made. The images or other third party material in this article are included in the article's Creative Commons licence, unless indicated otherwise in a credit line to the material. If material is not included in the article's Creative Commons licence and your intended use is not permitted by statutory regulation or exceeds the permitted use, you will need to obtain permission directly from the copyright holder. To view a copy of this licence, visit <http://creativecommons.org/licenses/by/4.0/>.

References

1. J.S. Lowengrub, H.B. Frieboes, F. Jin, Y.-L. Chuang, X. Li, P. Macklin, S.M. Wise, V. Cristini, Nonlinear modeling of cancer: bridging the gap between cells and tumors. *Nonlinearity* **23**, R1–R9 (2010). <https://doi.org/10.1088/0951-7715/23/1/r101>
2. C. Ehemann, S.J. Henley, R. Ballard-Barbash, E.J. Jacobs, M.J. Schymura, A.-M. Noone, L. Pan, R.N. Anderson, J.E. Fulton, B.A. Kohler, A. Jemal, E. Ward, M. Plescia, L.A.G. Ries, B.K. Edwards, Annual report to the nation on the status of cancer, 1975–2008, featuring cancers associated with excess weight and lack of sufficient physical activity. *Cancer* **118**(9), 2338–66 (2012). <https://doi.org/10.1002/cncr.27514>
3. B.A. Kohler, R.L. Sherman, N. Howlander, A. J, A.B. Ryerson, K.A. Henry, F.P. Boscoe, K.A. Cronin, A. Lake, A.-M. Noone, S.J. Henley, C.R. Ehemann, R.N. Anderson, L. Penberthy, Annual report to the nation on the status of cancer, 1975–2011, featuring incidence of breast cancer subtypes by race/ethnicity, poverty, and state. *J. Natl. Cancer Inst.* **107**(6), djv048 (2015). <https://doi.org/10.1093/jnci/djv048>
4. C. Letellier, S.K. Sasmal, C. Draghi, F. Denis, D. Ghosh, A chemotherapy combined with an anti-angiogenic drug applied to a cancer model including angiogenesis. *Chaos Solitons Fractals* **99**, 297–311 (2017). <https://doi.org/10.1016/j.chaos.2017.04.013>
5. I. Bashkirtseva, L. Ryashko, A.G. López, J.M. Seoane, M.A.F. Sanjuán, Tumor stabilization induced by T-cell recruitment fluctuations. *Int. J. Bifurc. Chaos* **30**, 2050179 (2020). <https://doi.org/10.1142/S0218127420501795>
6. M. Chi, A.Z. Dudek, Vaccine therapy for metastatic melanoma: systematic review and meta-analysis of clinical trials. *Melanoma Res.* **21**(3), 165–74 (2011). <https://doi.org/10.1097/CMR.0b013e328346554d>
7. A. Choudhury, S. Mosolits, P. Kokhaei, L. Hansson, M. Palma, H. Mellstedt, Clinical results of vaccine therapy for cancer: learning from a history for improving the future. *Adv. Cancer Res.* **95**, 147–202 (2006). [https://doi.org/10.1016/S0065-230X\(06\)95005-2](https://doi.org/10.1016/S0065-230X(06)95005-2)
8. W. Liu, T. Hillen, H.I. Freedman, A mathematical model for M-phase specific chemotherapy including the G_0 – phase and immunoresponse. *Math. Biosci. Eng.* **4**(2), 239–59 (2007). <https://doi.org/10.3934/mbe.2007.4.239>
9. I. Bashkirtseva, L. Ryashko, A.G. López, J.M. Seoane, M.A.F. Sanjuán, The effect of time ordering and concurrency in a mathematical model of hemoradiotherapy. *Commun. Nonlinear Sci. Numer. Simul.* **96**, 105693 (2021). <https://doi.org/10.1016/j.cnsns.2021.105693>
10. M. Itik, S.P. Banks, Chaos in a three-dimensional cancer model. *Int. J. Bifurc. Chaos* **20**, 71–79 (2010). <https://doi.org/10.1142/S0218127410025417>
11. L.G. de Pillis, A. Radunskaya, The dynamics of an optimally controlled tumor model: a case study. *Mathl. Comput. Model.* **37**, 1221–1244 (2003). [https://doi.org/10.1016/S0895-7177\(03\)00133-X](https://doi.org/10.1016/S0895-7177(03)00133-X)
12. A. López, J. Sabuco, J.M. Seoane, J. Duarte, C. Januário, M.A.F. Sanjuán, Avoiding healthy cells extinction in a cancer model. *J. Theor. Biol.* **349**, 74–81 (2014). <https://doi.org/10.1016/j.jtbi.2014.01.040>

13. P.E. Kloeden, E. Platen, *Numerical Solution of Stochastic Differential Equations* (Springer, Berlin, 2010)
14. I. Bashkirtseva, L. Ryashko, A.G. López, J.M. Seoane, M.A.F. Sanjuán, The effect of time ordering and concurrency in a mathematical model of chemoradiotherapy. *Commun. Nonlinear Sci. Numer. Simul.* (2021). <https://doi.org/10.1016/j.cnsns.2021.105693>